SSRG International Journal of Electronics and Communication Engineering
ISSN: 2348-8549/ https://doi.org/10.14445/23488549/IJECE-V13I8P104

Volume 13 Issue 8, 52-64, August 2026
© 2026 Seventh Sense Research Group®

Original Article

Design and Analysis of a Miniaturized Planar Triple-Band (28/38/43 GHz) Antenna with Hybrid-Ring Defected Ground Structure for 5G Applications

Souleymane BAH[1], Dominic KONDITI[2], Jeremiah ABOLADE[3], Robert MACHARIA[4]

[1]*Department of Electrical Engineering, Pan African University Institute for Basic Sciences, Technology and Innovation, hosted at Jomo Kenyatta University of Agriculture and Technology, Nairobi, Kenya*

[2]*College of Electrical and Electronic Engineering, Faculty of Engineering and Built Environment, Technical University of Kenya (TU-K), Nairobi, Kenya*

[3]*Department of Electrical Engineering, Pan African University Institute for Basic Sciences, Technology and Innovation, hosted at Jomo Kenyatta University of Agriculture and Technology, Nairobi, Kenya. / Department of Electrical/Electronic Engineering, Bowen University, Iwo, Nigeria.*

[4]*Department of Telecommunication and Information Engineering, School of Electrical, Electronic, and Information Engineering, Jomo Kenyatta University of Agriculture and Technology (JKUAT), Nairobi, Kenya.*

[1]*Corresponding Author : souleymane.bah@students.jkuat.ac.ke*

Received: 08 May 2026 Revised: 11 June 2026 Accepted: 15 July 2026 Published: 31 August 2026

Abstract *- This article describes a compact planar microstrip patch antenna with tri-band functionality at 28 GHz, 38 GHz, and 43 GHz, suitable for 5G millimeter-wave applications. By incorporating a 43 GHz band, the antenna covers additional high-frequency applications like high-capacity backhaul and upcoming B5G/6G systems. The design uses a Hybrid-Ring Defected Ground Structure (HR-DGS) in combination with a slot-loaded radiating patch, which facilitates better control of surface current distribution and multiple resonant modes in a miniaturized design. The antenna uses a Rogers RT/Duroid 5880 substrate, which has εr = 2.2 and tan δ = 0.0009, providing low dielectric loss at high frequencies. The electromagnetic design simulations were carried out in ANSYS HFSS and confirmed the triple-band operation with reflection coefficients of −22.56 dB, −23.49 dB, and −14.43 dB at 28 GHz, 38 GHz, and 43 GHz, respectively. CST Microwave Studio was used to verify the simulated S-parameter response. The simulated gains at the three operational bands were 6.33 dBi, 4.20 dBi, and 4.71 dBi, with the radiation efficiencies of 87.11%, 84.30%, and 89.12%, indicating good performance for the specified frequency bands. The antenna is just 4 × 5 × 0.787 mm³. The combination of size, the simplicity of the HR-DGS design, and the antenna's improved multiband functionality and surface-wave suppression makes it a suitable solution for 5G millimeter-wave systems.*

Keywords *- Triple-band antenna, Microstrip patch antenna, Millimeter-wave, 5G Applications, Hybrid-Ring Defected Ground Structure.*

1. Introduction

The rapid development of wireless Fifth-Generation (5G) networks has created a demand for smaller and more efficient antennas that can operate reliably at mmWave frequencies. The 3rd Generation Partnership Project (3GPP) established that the 28 GHz and 38 GHz frequencies, in Frequency Range 2 (FR2), can provide enhanced mobile broadband, ultra-low latency, and highly-dense Internet-of-Things (IoT) services. In addition, the 43 GHz band is attracting attention for applications such as high-capacity wireless backhaul, Fixed Wireless Access (FWA), and satellite communications in the Q/V bands, as well as for B5G/6G systems. Moreover, recent studies found that Defected Ground Structures (DGS) offer a solution to the challenges of higher-frequency operation by adding new resonance structures through the controlled alteration of surface currents. Challenges remain for mmWave systems. These include high free space path loss and the limited bandwidth of mobile and IoT devices that require smaller and more efficient designs. These challenges fuel the designs of efficient, compact, multiband antennas that function reliably across multiple frequency bands. Because of their planar profile, low weight, ease of fabrication, and PCB compatibility [4], microstrip antennas work well for mmwave applications. However, traditional, single-layer microstrip antennas are often limited to a single operating frequency or have a very small bandwidth.

They also have low efficiency in small forms. To overcome such challenges, Defected Ground Structures (DGS) have been implemented. By introducing engineered discontinuities in the ground plane of the antenna, DGS can change the distribution of surface currents, reduce the effect of surface waves, improve the matching of surface currents, and offer a multiband operation, all without significantly increasing the complexity of the fabrication process [5, 6].

2. Related Works

Several microstrip antenna designs for millimeter-wave 5G applications have been presented in the recent literature.

Al-Atyar et al. (2025) [1] introduced a dual-band patch antenna provisioned for the 28 GHz and 38 GHz bands. The compact design of the antenna enables good matching and supports communications in the FR2. The design, however, is limited to dual-band, and thus, missing the 43 GHz band limits the design for multi-band, millimeter-wave systems.

Elsharkawy et al. (2023) [4] designed a dual-band MIMO antenna of a compact form. The antenna supports millimeter-wave applications and offers high gain and diversity. The design is hence suitable for next-generation 5G communications. The MIMO design, however, inherently increases the complexity of the antenna design as compared to a single-element antenna.

Khan et al. (2024) [5] introduced a dual-band MIMO antenna using a metamaterial. The design improves the isolation between the MIMO elements and enhances the performance of the antenna. The overall complexity of the metamaterial MIMO design also increases compared to a microstrip design.

Frist et al. (2024) [6] introduced a CSRR-based MIMO antenna with a DGS and reconfiguration capability. The design offers flexibility in tuning, thus versatile for varying communications. The design, however, increases the complexity of the overall system due to the circuitry provisioned for the reconfiguration.

Bhadravathi Ghouse et al. [7] (2024) designed a dual-band, 28 GHz and 38 GHz, slot-loaded antenna for millimeter-wave 5G and beyond. The authors highlighted the antenna's simple structure and its enhanced bandwidth due to slot perturbation. Nevertheless, this design exclusively operates in dual-band, with no provisions for other bands, such as 43 GHz.

Ullah et al. [8] (2022) designed a pixelated antenna equipped with Defected Ground Structure (DGS) for narrow-band wireless and IoT applications. The antenna is low-profile and well-suited for small-size constraining applications. However, the design of the pixelated DGS structure is likely to be complicated and time-consuming, due to the intensive nature of the optimization process.

Kumar et al. [9] (2023) developed a DGS-based MIMO antenna array for millimeter-wave communications. The array achieved excellent performance for 5G applications, as it exhibited a wide bandwidth and high gain. However, it also exhibited a large size and high complexity of fabrication due to its multi-element MIMO configuration.

Diallo et al. [10] (2023) designed a compact dual-band antenna with a square-ring DGS that combines 5G and sub-6 GHz applications. The proposed design is compact and dual-band. However, the design is limited to dual-band.

Anooz et al. [19] (2023) developed a rectangular microstrip patch antenna for microwave applications with a G-shaped slot. Designed and simulated via CST, the antenna operates at 7.51 GHz, 8.01 GHz, and 10.68 GHz. The simplicity in structure, good return loss values, and 97.35% efficiency made this work advance considerably. The created antenna does not fall in the 5G mmWave bands, and covers neither 28 GHz, 38 GHz, nor 43 GHz, and the research was largely based on simulations.

Tiwari et al. [18] (2025) studied a 24 GHz, 28 GHz, and 38 GHz four-port MIMO antenna designed for millimeter-wave wearable applications. The antenna displays excellent isolation (greater than 20 dB), gain, and radiation efficiency (greater than 82%), and has bending, SAR, and link-margin analyses included. The main drawback of this work is a larger and more complex design. Due to the four-port design, the antenna structure is not suitable for compact single-element antenna integration.

Gaid and Ali [17] (2023) developed a compact tri-band antenna of the rectangular microstrip patch variety for 5G applications at 28, 38, and 60 GHz, utilizing a π-shaped slot. The antenna was optimized in HFSS and had a good gain, bandwidth, and radiation efficiency after validation in CST. The antenna cannot cover the 43 GHz band, and the authors included no fabrication or measurements for the study.

Promising results have come from these studies, but many of these designs depend on multilayer substrates, MIMO configurations, or intricate resonator structures that make fabrication and the overall antenna size more complex.

In addition, most existing compact antennas are designed primarily for dual-band operation at 28 and 38 GHz. Compact antennas that are single-element and that can operate at 28, 38, and 43 GHz are even more difficult to find.

Table 1. Studies in the literature

Reference	Antenna Design/ Method	Strengths	Limitations
Al-Atyar et al. [1] (2025)	Dual-band loaded patch antenna (28/38)	Compact structure, good impedance matching; suitable for FR2 applications.	Limited to dual-band operation; does not support the 43 GHz band.
Elsharkawy et al. [4] (2023)	Dual-band compact MIMO antenna	High gain and diversity performance; suitable for high-capacity systems	Increased design complexity due to MIMO configuration
Khan et al. [5] (2024)	Metamaterial-based dual-band MIMO antenna.	Enhanced isolation and coupling reduction performance.	Requires metamaterial structures, increasing fabrication complexity
First et al. [6] (2024)	Reconfigurable antenna using CSRR and DGS	Radiation pattern reconfigurability	Additional control circuitry is required.
Bhadravathi Ghouse et al. (2024) [7]	Slot-loaded dual-band antenna	Simple structure; improved bandwidth	Supports only 28/38 GHz bands
Ullah et al. [8] (2022)	Pixelated DGS antenna	Compact profile; IOT suitability.	Computationally intensive
Kumar et al. [9] (2023)	DGS-based MIMO antenna array	High gain; wide bandwidth	Large size and fabrication complexity
Diallo et al. [10] (2023)	Square-ring DGS dual-band antenna	Miniaturized structure	No triple-band operation, no fabrication.
Anooz et al. [19] (2023)	Rectangular microstrip patch antenna with G-shaped slot, designed using CST for 7.51, 8.01, and 10.68 GHz	Simple structure; tri-band operation; good return loss; high efficiency of about 97.35%	Not designed for 28/38/43 GHz 5G mmWave bands; only CST simulation; no fabrication reported
Tiwari et al. [18] (2025)	Flexible 4-port MIMO antenna for 24/28/38 GHz using Rogers RO3003 substrate	Fabricated and measured; good isolation >20 dB; high gain up to 8.48 dBi; bending and SAR analysis included	Larger size due to 4-port MIMO structure; more complex than single-element antennas
Gaid and Ali [17] (2023)	Compact tri-band rectangular patch antenna with π-shaped slot for 28/38/60 GHz, optimized in HFSS and verified with CST	Compact size; tri-band 5G operation; good gain and efficiency; HFSS/CST validation	No fabrication or measurement; 43 GHz band not covered; radiation direction changes at higher bands
This Work	Quad-slot patch with Hybrid-Ring DGS	Compact size (4×5×0.787 mm^3 triple-band operation (28/38/43 GHz); good impedance matching validated by HFSS and CST	Fabrication and measurement remain for future work

Thus, there is still an opportunity to create highly miniaturized, low-complexity, and single-layer triple-band antennas that are designed with the goal of stable operation across several millimeter-wave frequency bands and that can also maintain good performance with respect to bandwidth, gain, and radiation efficiency. The present work addresses this gap through the integration of a quad-slot radiating patch and a Hybrid-Ring Defected Ground Structure (HR-DGS), enabling compact triple-band operation at 28 GHz, 38 GHz, and 43 GHz.

An efficient, compact planar microstrip antenna, using a Hybrid-Ring Defected Ground Structure (HR-DGS), has been introduced to tackle some of the challenges in the field.
The proposed structure develops the ground current on the HR-DGS and the concentric circular and square slot geometries. The gaps in the ring form the radiating patch, and the proposed structure effectively creates current paths that resonate and enable reliable, compact triple-band operation at the specified frequency ranges (i.e., 28, 38, and 43 GHz). The proposed antenna has been analyzed using ANSYS HFSS. The S-parameter of the proposed antenna has also been tested and verified in CST Microwave Studio.

The design and effectiveness of the proposed structure were validated using full-wave electromagnetic simulations in ANSYS HFSS. The antenna achieved triple-band reliability with return losses of −22.56 dB and −23.49 dB at 28 GHz and at 37.938 GHz, respectively, and −14.43 dB at 43 GHz, all less than −10 dB.

Furthermore, the total area for the structure was achieved at 4 mm x 5 mm. Compared to other antenna designs that are multilayered and are therefore more complicated, the proposed antenna structure is fully planar and integrates the benefits of the hybrid-ring ground modification. It can easily integrate into other 5G, B5G, and IoT platforms.

To the best of the authors' knowledge, few compact single-layer and single-element microstrip antennas have been reported for simultaneous operation at 28 GHz, 38 GHz, and 43 GHz for 5G millimeter-wave communication. The three bands are achieved in a compact size of 4 × 5 × 0.787 mm³, without the use of multilayer substrates, large MIMO configurations, or complicated resonator structures, frequently employed in other designs. Also, this work proposes a quad-slot radiating patch combined with a Hybrid-Ring Defected Ground Structure (HR-DGS) for a novel design approach.

The quad slots create the added resonating modes at 38 and 43 GHz, and the HR-DGS provides enhancement of impedance matching, bandwidth, and radiation stability without growing the antenna. Additionally, this design implements two independent full-wave Electromagnetic (EM) simulations for verification.

The two independent full-wave EM simulations are ANSYS HFSS and CST Microwave Studio, and the results of the two simulations show excellent agreement. The design is compact and demonstrates stable triple-band operation and excellent electromagnetic performance; therefore, the design is novel.

3. Antenna Design Methodology

3.1. Mathematical Design Model and Antenna Specifications

To determine the preliminary dimensions of the proposed antenna radiator, the transmission line model was used. [12] The Width (Wp) and Length (Lp) of a microstrip antenna can be determined through empirical equations that consider a few factors that include the operating Frequency (fr), the height of the Substrate (h), and the substrate's Relative Permittivity (εr).

In this case, the first patch was assumed to operate at 28 GHz, using Rogers RT/duroid 5880 (εr = 2.2, tan δ = 0.0009), and as a first step, an antenna structure was defined on a ground plane (size: 9.2 mm x 8.8 mm), as shown in Figure 1. All the following iterations and optimizations took into account the results of those first approximations to achieve multi-frequency operation of the antenna and its miniaturization.

To compute the length and width of rectangular patch antennas, use the following equations.

$$W = \frac{c}{2f_0\sqrt{\frac{\varepsilon_r+1}{2}}} \tag{1}$$

Where c is the speed of light, ε_r represents the dielectric constant and f_0 Is the resonance frequency. When the antenna radiates, part of the electromagnetic wave travels through the air while another portion penetrates the substrate and reaches the ground plane. Because the dielectric constants of air and the substrate differ, an Effective Dielectric Constant (ε_{eff}) must be used. It can be computed using the corresponding formula.

$$\varepsilon_{eff} = \frac{\varepsilon_r+1}{2} + \frac{\varepsilon_r-1}{2}\left[1+\frac{12h}{W}\right]^{-1/2} \tag{2}$$

Here, h represents the thickness of the substrate. The patch length can then be calculated using the following equation.

$$L = \frac{c}{2f_0\sqrt{\varepsilon_{eff}}} \tag{3}$$

Because of fringing effects, the antenna's electrical length increases by an amount ΔL. The extended patch length is given by:

$$\Delta L = 0.412\frac{(\varepsilon_{eff}+0.3)(\frac{W}{h}+0.254)}{(\varepsilon_{eff}-0.258)(\frac{W}{h}+0.8)} \tag{4}$$

Equations (5) and (6) are used to calculate the minimum required length ($\boldsymbol{L}_{\text{sub}}$) and width ($\boldsymbol{W}_{\text{sub}}$) of the substrate.

$$L_{sub} = 6h + L \tag{5}$$

$$W_{sub} = 6h + W \tag{6}$$

3.2. Antenna Design Strategy

Designing the proposed antenna utilized a two-step iterative model for multi-band design. Each step of the design was implemented and examined using ANSYS HFSS and CST Studio to corroborate S-parameter results. The size and shape of the radiating elements were refined systematically over the subsequent iterations to accommodate additional operating bands to the antenna bandwidth.

3.2.1. Initial Antenna Configuration

As shown in Figure 2, the initial design incorporates a standard rectangular microstrip patch antenna tuned to resonate at 28 GHz. The patch was designed on a Rogers RT/Duroid 5880 substrate with initial dimensions of 9.2 mm × 8.8 mm, while the ground plane remained unchanged at this stage.

It should be noted that the 9.2 mm × 8.8 mm dimension corresponds only to the initial antenna configuration, whereas the final optimized structure was reduced to a compact volume of 4 × 5 × 0.787 mm³. This initial configuration served as a reference structure for subsequent design improvements, leading to the proposed triple-band microstrip patch antenna.

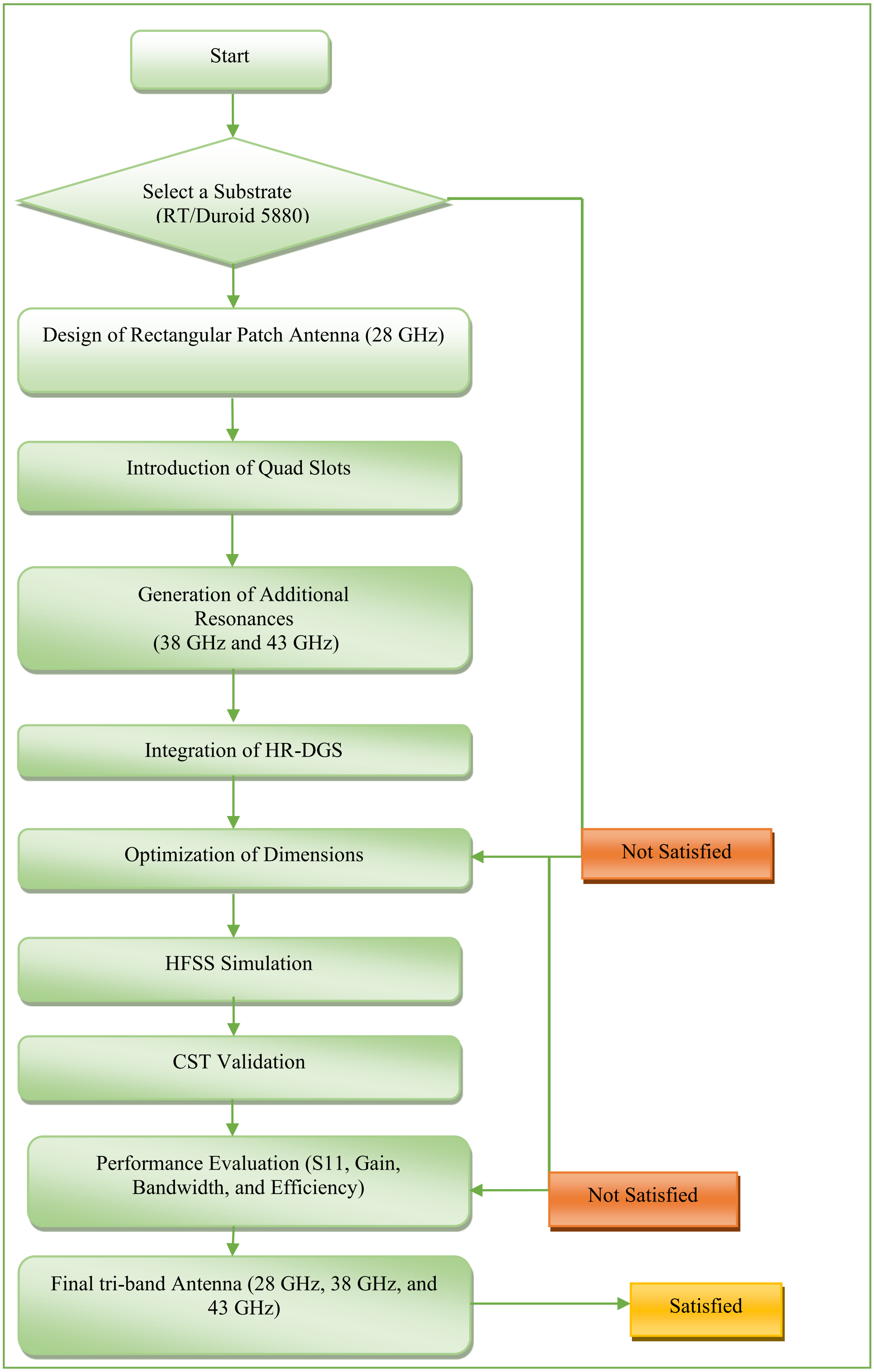

Fig. 1 Design methodology and optimization workflow of the proposed triple-band microstrip antenna

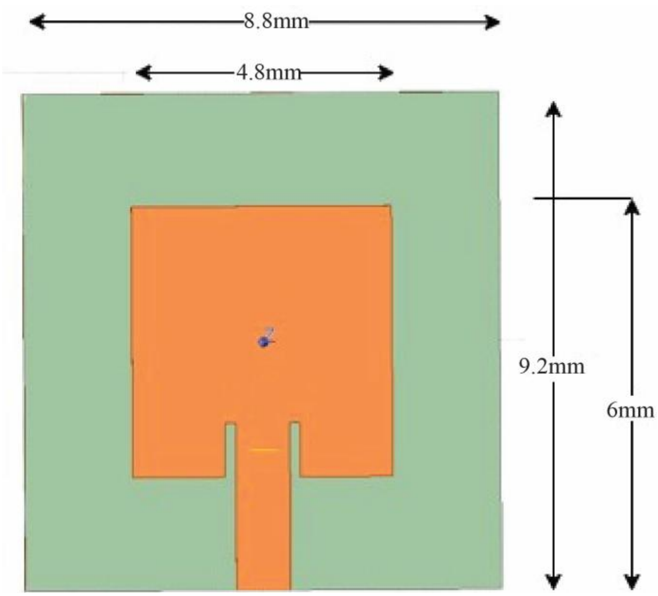

Fig. 2 Top part of the initial antenna at 28 GHz

Step 1: Multiband Excitation and Miniaturization.

3.2.2. Introduction of Quad Slots

To widen the frequency band, quad slots were incorporated into the radiating patch, seen in Figure 3. Creating more current paths, this patch design modification extends the effective physical length of the antenna, thereby significantly modifying the antenna's electromagnetic performance. This results in multiple resonant modes being excited, yielding additional bands of 38 GHz and 43 GHz. Bands of this nature are important to millimeter wave 5G. These modes provide further resonances and increase electromagnetic coupling. At this stage, only small impedance mismatches can be noted.

3.2.3. Final Optimized Design.

In the final design stage, the Hybrid-Ring Defected Ground Structure (HR-DGS) was introduced into the ground plane, as in Figure 5. The HR-DGS produces a controlled perturbation of the ground current distribution and modifies the equivalent inductive coupling of the antenna. This effect increases the effective electrical path, improves impedance matching, reduces surface-wave effects, and stabilizes the resonances at the target bands. It is important to note that the additional resonances at 38 GHz and 43 GHz are mainly produced by the quad-slot radiating patch, while the HR-DGS primarily enhances impedance matching, bandwidth, and overall radiation stability. Therefore, the combination of the quad-slot patch and HR-DGS enables compact and stable triple-band operation at 28 GHz, 38 GHz, and 43 GHz.

3.2.4. Parametric Optimization and Miniaturization

An investigation into the most useful slot size was conducted. This allows for better management of the resonant frequency with the assurance of stable performance at 28 GHz, 38 GHz, and 43 GHz. Also, adjusting the flow path of the current aids in miniaturizing the antenna, which results in a 4 mm x 5 mm compact design.

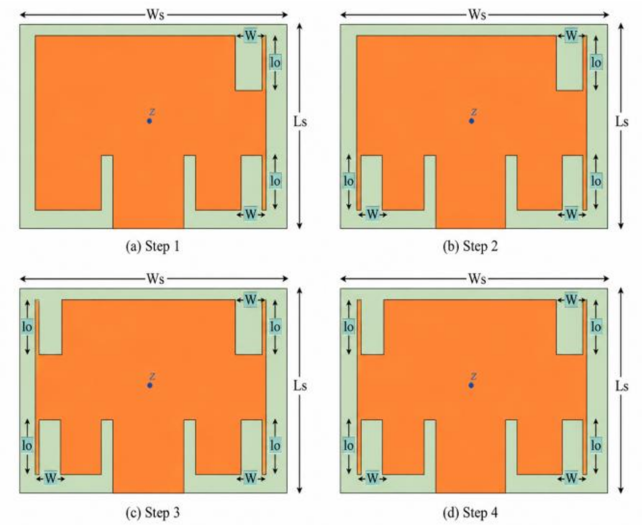

Fig. 3 Antenna design evolution from Step 1 to Step 4

Step 2: Performance Enhancement and Final Optimization

As represented in Figure 5, at the last design phase, the Hybrid-Ring Defected Ground Structure (HR-DGS) is integrated into the antenna's design and is proven to play a significant part in the overall enhancement of antenna performance in the electromagnetic spectrum.

The HR-DGS causes a designed disturbance in the ground plane, which modifies the surface current distribution and changes the inductive-capacitive (LC) coupling. The disturbance creates longer electrical paths and increases the electromagnetic coupling between the radiating patch and the ground plane. It should be noted that the HR-DGS does not create new resonant frequencies.

The extra resonant modes at 38 GHz and 43 GHz are due to the slot-loaded radiating patch, which creates several current paths and promotes higher-order resonant modes. The enhancement of the system's overall performance is the main purpose of the HR-DGS.

The HR-DGS's impact on impedance matching is two-fold: first, by controlling the return current on the ground plane, and second by reducing the dispersion of surface waves.

Both lead to bandwidth expansion and resonance stabilization at high frequencies. Also, the design uses a combination of square and circular slots, which allows the dispersion of return current more than conventional DGS.

This also improves the radiation of the structure without increasing dimensions. The described characteristics allow the design of a compact, efficient, and stable multi-band antenna that operates in the millimeter-wave 5G region.

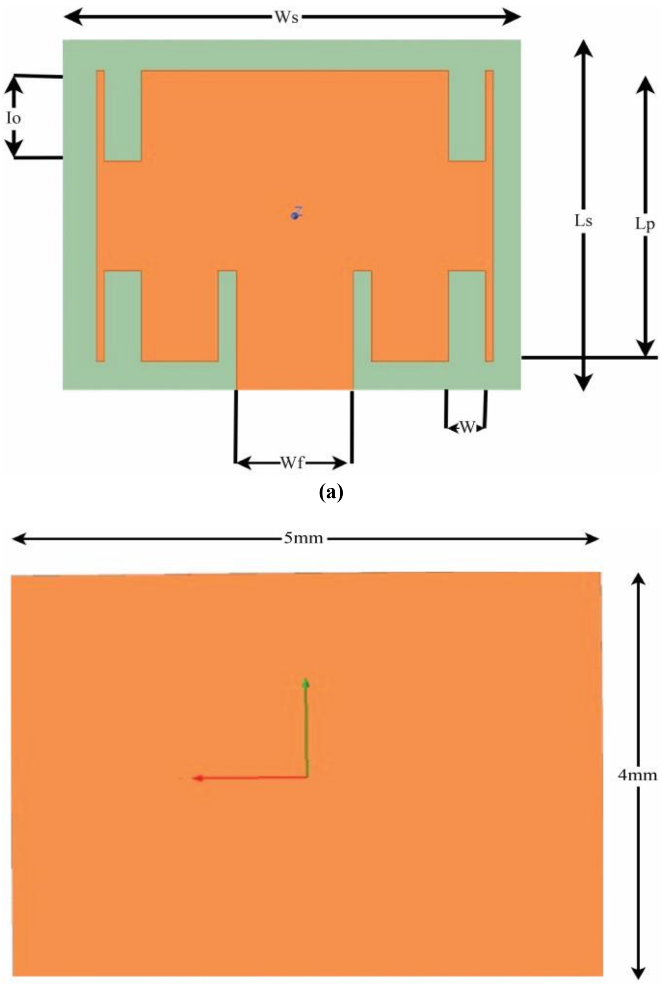

(b)

Fig. 4 Structure of first stage antenna, (a) Top view, (b) Bottom view

4. Results and Discussion

This section presents and discusses the simulated performance of the proposed Hybrid-Ring DGS antenna. The analysis focuses on the reflection coefficient, bandwidth, gain, radiation efficiency, radiation patterns, and comparison with previous works. The S-parameter response obtained from ANSYS HFSS is also compared with CST Microwave Studio results to verify the triple-band behavior of the proposed antenna.

Table 2. Parameters of recommended microstrip patch antenna

Parameter	Value(mm)	Parameter	Value(mm)
Ls	4	**Wf**	1.25
Ws	5	**D1**	1
Lg	4	**D2**	0.9
Wg	5	**D3**	0.6
mt	0.035	**D4**	0.46
hs	0.787	**Wsq**	1.8
Lp	3.3	**Wsq2**	1.7
Wp	4.26	**lw**	0.2

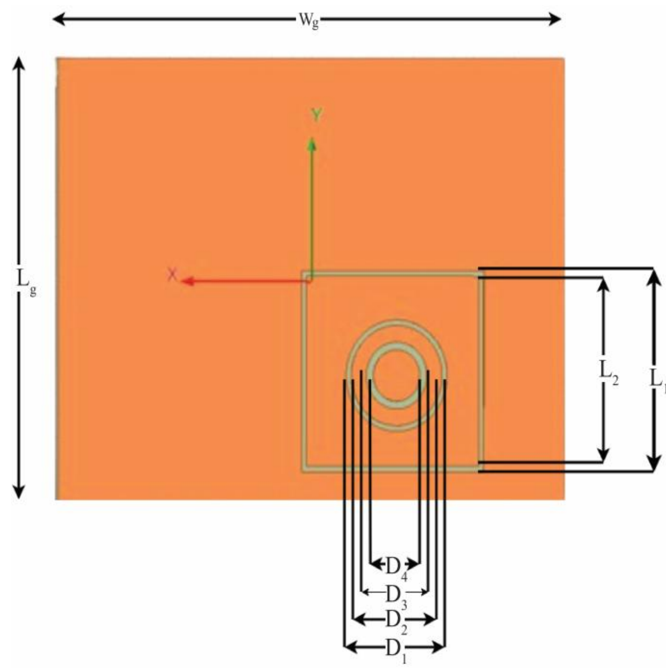

Fig. 5 Bottom view of final antenna

4.1. Reflection Coefficient (S_{11})

Using full-wave EM simulations in ANSYS HFSS, we analyzed the antenna's performance. The evolution of the simulated S11 response at different design stages is illustrated in Figure 6, while the final antenna performance is summarized in Table 3 at different phases.

As shown in Figure 5, the antenna initially had a resonant frequency of 28 GHz and exhibited poor impedance matching. The use of quad slots produced two more resonances at around 38 GHz and 43 GHz, implying that the antenna is capable of multiple operational modes. With the use of the HR-DGS structure, the antenna achieved deeper S11 minima, improved impedance matching, and more stable performance across the three frequency regions.

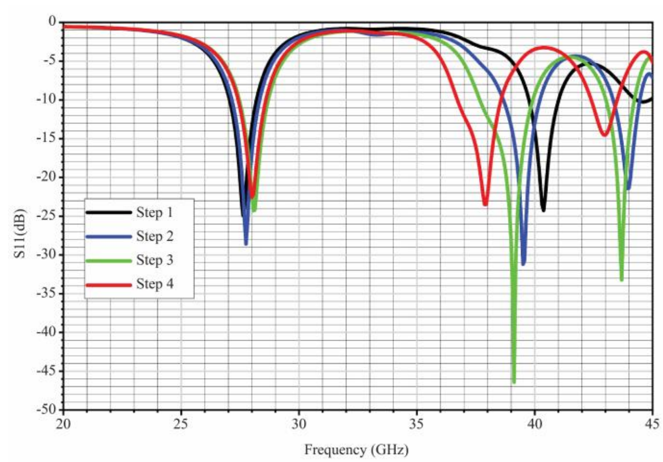

Fig. 6 Simulated reflection coefficient (S_{11}) of the antenna at different design stages: initial structure, Slot-loaded configuration, and the final optimized with HR-DGS

4.2. Parametric Analysis

A parametric study was carried out on certain main factors to achieve the needed frequency bands across a wide range and to optimize impedance matching. This part analyzes how the performance of the antenna being proposed is affected by the following factors: Slot Length (lo), Slot Width (W), and Inset Gap Width (lw). The performance of the antenna is affected by the optimization of these factors, among others.

4.2.1. Effects of Slot Length (lo)

Referenced in Figure 7, adjusting the Slot Length (lo) from 0.97 mm to 1.024 mm displays a significant effect on the antenna characteristics. For larger values of lo, the resonant frequency shifts downwards because of the active length extension, and for smaller values of lo, the resonant frequency shifts upwards. Increasing or decreasing the lo value also impacts the impedance matching, demonstrated through changes in the depth of S11 minima. From the figure, we can say the optimal value of lo is in the interval of 1.01 to 1.02 mm. It can hence be stated that lo acts mostly as a tuning parameter.

4.2.2. Effects of Slot Width (W)

In Figure 8, it can be seen that the optimal range of adjusting the gap width between the inset arms of the proposed antenna, from 0.36 mm to 0.4 mm, provides the best impedance matching performance with negligible shifts in the resonant frequencies of 28 GHz, 38 GHz, and 43 GHz.

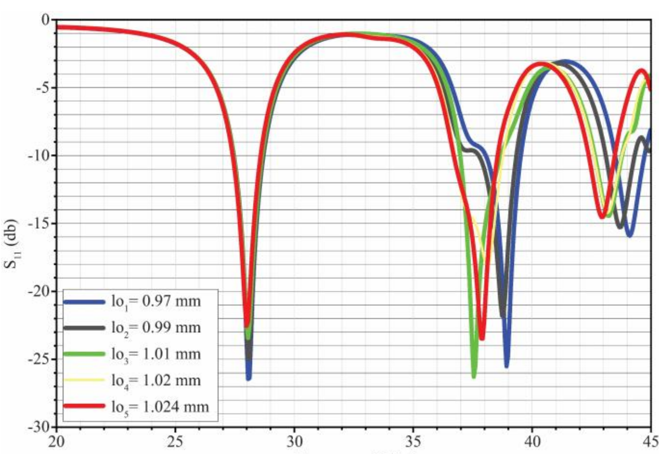

Fig. 7 Effect of slot length (lo) on the S11 performance

The first resonant frequency (28 GHz) demonstrates minimal variation and little reliance on W, with slight variation in return loss. The second (38 GHz) and third (43 GHz) resonant frequencies appear to rely more on the feeding mechanism.

The second resonant frequency, at 38 GHz, has an improved minimum return loss at W = 0.36 mm, but this value is still outside the specified frequency range. Then, W = 0.4 mm, which gives a worse return loss, is an improvement and places the frequency closer to the target 38 GHz. It is therefore reasonable to assume that W = 0.4 mm provides a better impedance matching solution and major return loss constraints for the antenna.

4.2.3. Effects of Inset Gap Width (lw).

The diagram in Figure 9 illustrates that adjusting the Inset Gap Width (lw) between 0.2mm and 0.5mm has an insignificant effect on the resonant frequencies, which stay roughly constant around 28 GHz, 38 GHz, and 43 GHz. For example, lw = 0.2 mm already places the resonances along the target frequencies. On the other hand, lw alters the S11 notch depth and, thus, the impedance matching.

However, of all the chosen values, lw = 0.3 represents the ideal overall solution, with the most pronounced and well-balanced resonances across the complete range. This behavior suggests that lw is primarily an impedance matching parameter instead of an adjustable frequency parameter.

4.3. Bandwidth and Resonance Characteristics Summary

a) 28 GHz Band: At 28 GHz, the antenna resonates with an S_{11} of -22.56 dB, where the impedance bandwidth increased slightly from 1.13 GHz to 1.19 GHz following the HR-DGS integration.

b) 38 GHz Band: At 38 GHz, a deep resonance is observed at 37.938 GHz with an S_{11} of -23.49 dB. A significant enhancement was observed here, where the bandwidth expanded substantially from 0.9 GHz to 1.87 GHz, demonstrating the strong influence of the HR-DGS on higher-order resonance stabilization.

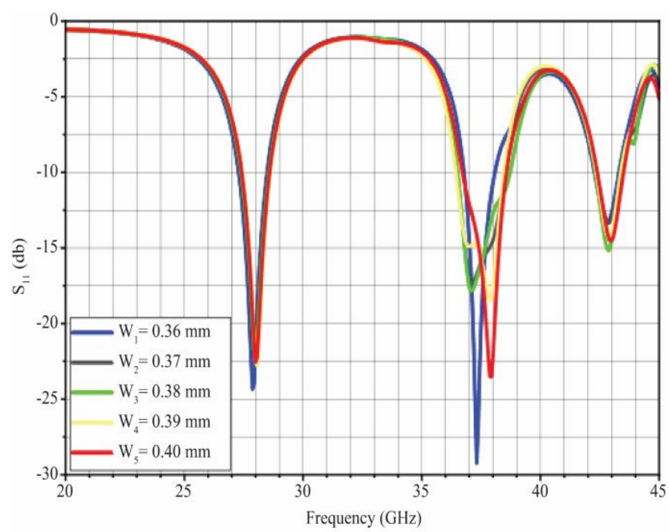

Fig. 8 Effect of slot width (W) on the S11 performance

c) 43 GHz Band: At 43 GHz, a resonance occurs at 43 GHz with an S_{11} of -14.43 dB, where the bandwidth improved from 0.75 GHz to 1.12 GHz.

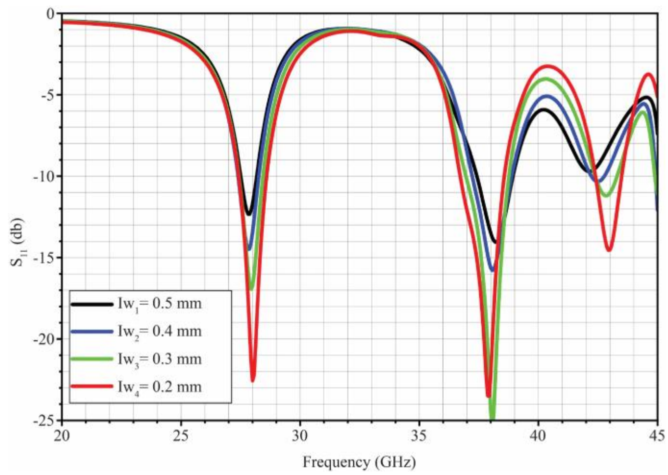

Fig. 9 Effect of inset gap width (lw) on the S11 performance

Table 3. Simulation results of the proposed antenna at 28 GHz, 38 GHz, and 43 GHz

Frequency (GHz)	S11	VSWR	BW (GHz)	Gain (dBi)	Directivity (dB)	Efficiency %
28	-22.56	1.29	1.19	6.33	6.38	87.11
37.938	-23.49	1.16	1.87	4.20	4.28	84.30
43	-14.43	1.8	1.12	4.71	4.75	89.12

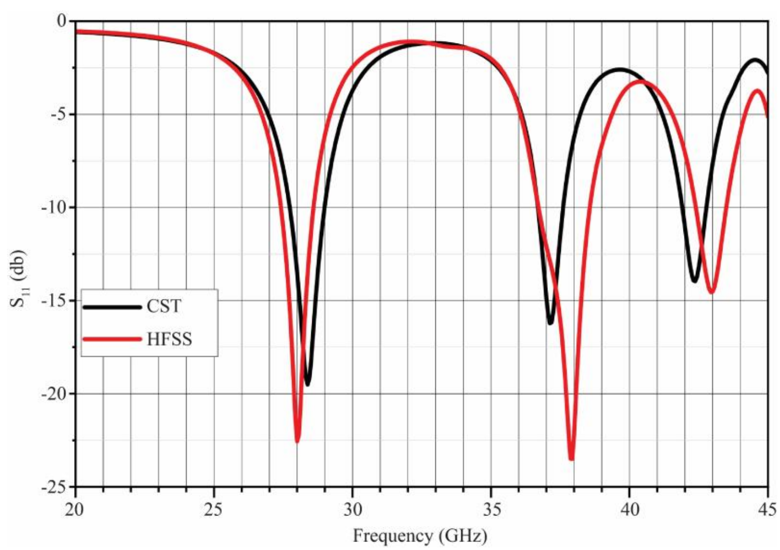

Fig. 10 Comparison of simulated reflection coefficient (S11) for the proposed antenna using CST and HFSS

4.4. HFSS and CST S-Parameter Comparison

Simulations of the proposed antenna's reflection coefficient (S11) using CST and ANSYS HFSS are shown in Figure 10. The antenna simulations from both methods validate the multiband nature of the antenna and good impedance matching.

The HFSS simulation results show that the antenna resonates at 28 GHz, 37.938 GHz, and 43 GHz with the following lower resonance levels of -22.56 dB, -23.49 dB, and -14.43 dB, respectively.

Conversely, the CST simulation establishes resonances at marginally higher frequencies. However, the return loss values are similar to those from the HFSS Simulation. These discrepancies can be attributed to the different nature of the simulation algorithms, especially the meshing and solvers used in CST and HFSS. Even though this discrepancy exists, both Simulation techniques show great confidence in the suggested antenna. The results also show considerable bandwidth available at all resonances, with the most significant resonance seen at 38 GHz.

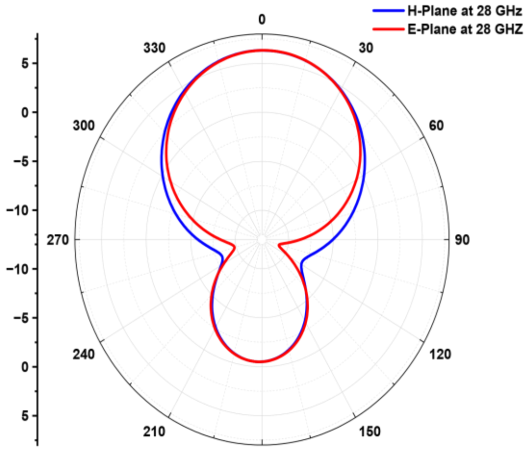

(a)

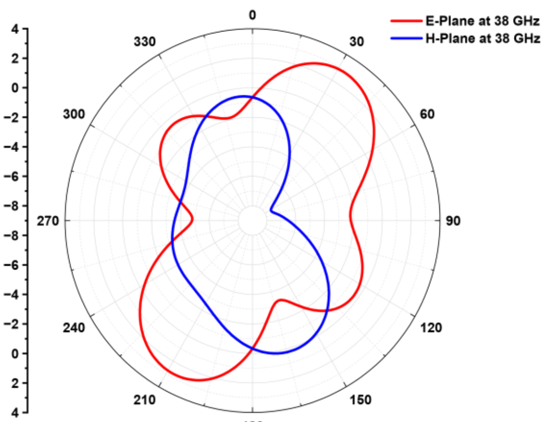

(b)

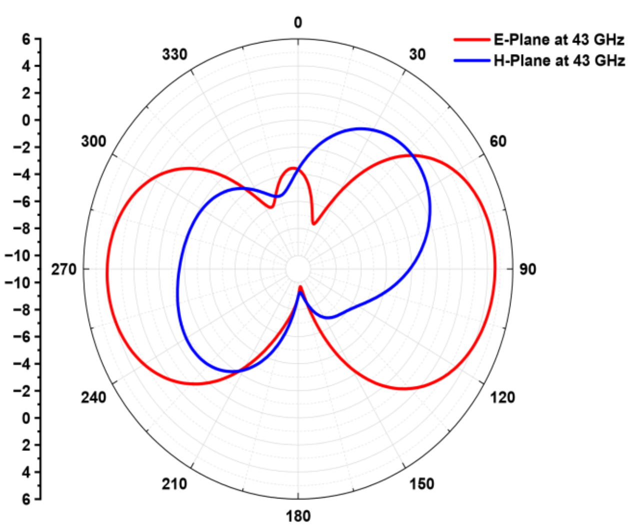

(c)

Fig. 11 2D radiation pattern for both H and E plane at, (a) 28 GHz, (b) 38 GHz, and (c) 43 GHz.

4.5. Far-field 3D Radiation Characteristics

E-plane and H-plane radiation patterns for the proposed antenna at 28 GHz, 38 GHz, and 43 GHz are depicted in the above figures. They describe the antenna's 2D radiation characteristics at each of the millimeter-wave frequency bands, specifying every azimuth and elevation. At 28 GHz, the antenna confirms the modal pattern characteristics of microstrip rectangular patch antennas exhibiting broad-pattern microstrip antenna behavior at 28 GHz in both the E and H planes.

The E-plane and H-plane radiation patterns exhibit a microstrip antenna behavior pattern. The H-plane radiation pattern is almost symmetric with minimal back lobe. The E-plane radiation pattern exhibits a dipole radiation pattern with a back lobe, a null, and a main lobe. The dipole behavior suggests low radiation side lobes and a well-defined radiation pattern, indicating the primary mode of the antenna is supported, and the radiation is stable.

At 38 GHz, the antenna exhibits a deliberate change in its radiation behavior. Compared with 28 GHz, the radiation pattern is more 2D, more focused, and more directive, as evidenced by a narrowing of the main lobe, with less back lobe. The radiation behavior is primarily broadside. The side lobe patterns in the H and E-plane radiation patterns indicate a modest level of radiation asymmetry. The radiation and polarization characteristics remain acceptable for applications in the millimeter-wave region.

The antenna demonstrates a more complex radiation pattern at 43 GHz as it becomes more directive. The primary lobe is held perpendicular, but multiple other lobes with significant angular variations appear. This is typical of higher frequencies as the patch becomes larger in terms of wavelength, leading to higher-order effects in the current distribution on the patch. The antenna still maintains a high level of forward directional dominance with a good F/B ratio. The fact that the radiation patterns become stable in all three operating bands suggests that the design of the antenna achieves a good level of multi-band performance while maintaining the in-line broadside properties required in 5G mmWave communication systems.

4.6. Far-field 3D Radiation Characteristics

3D radiation analysis shows the antenna operates optimally in broadside mode at 28 GHz. As a result, the antenna displays an effective radiation pattern with a sharp increase in gain. At 38 GHz and 43 GHz, the antenna shows complex radiation behavior, including multi-lobe structures caused by higher-order resonances. Despite the multi-lobe structures at 38 GHz and 43 GHz, the antenna maintains a dominant pattern of radiation in the forward direction across all bands. This confirms that the antenna is appropriate for multi-frequency millimeter-wave communication systems.

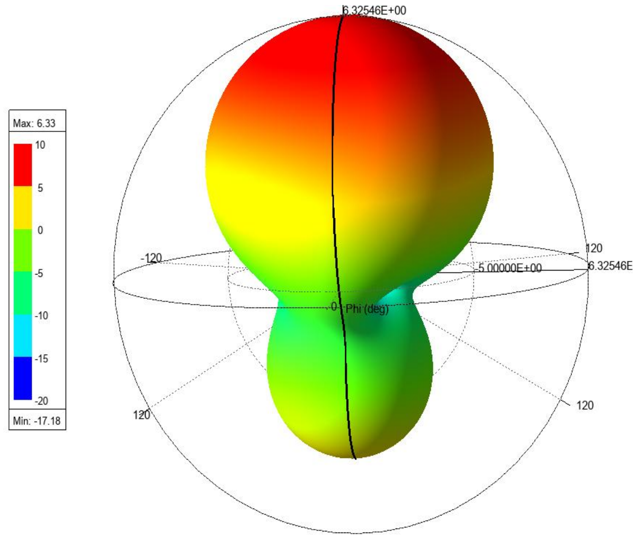

(a)

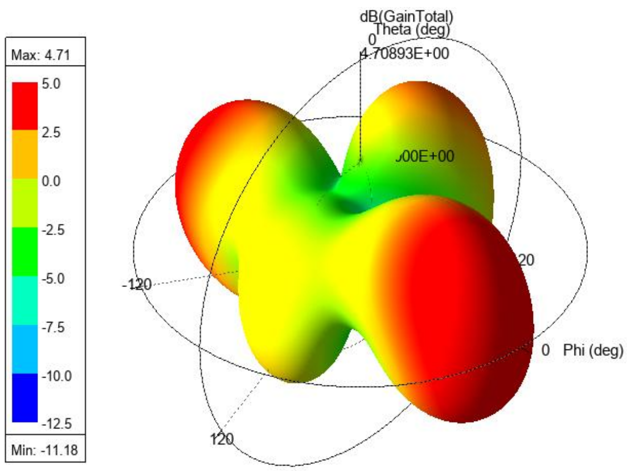

(b)

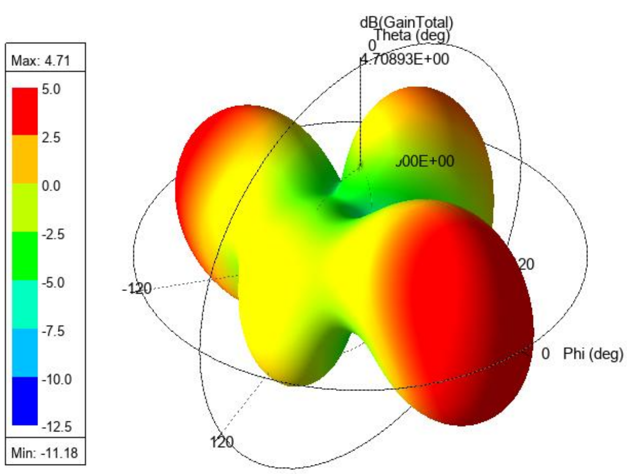

(c)

Fig. 12 3D far-field radiation patterns of the proposed antenna (dBi) at (a) 28 GHz, (b) 38 GHz, and (c) 43 GHz.

The proposed antenna is more compact than other previously documented designs while exhibiting more competitive gain and bandwidth. There is a trade-off among peak gain at higher frequencies, the antenna's compactness, constant impedance matching, and multi-band functionality. Some of the designs mentioned in the literature achieve a higher gain, although this typically comes at the expense of added dimensions to the structure and/or an increased number of layers. The research presented here indicates that the proposed antenna based on HR-DGS stands out as an excellent choice for compact 5G millimeter-wave communication devices and IoT systems, where the small size of the structure, low cost of systems, and high radiation efficiency are the most critical issues.

4.7. Radiation Efficiency

The radiation efficiency results reveal that the antenna sustains efficiency over the entire frequency range. Specifically, the efficiency levels were 87.11% at 28 GHz, 84.30% at 38 GHz, and 89.12% at 43 GHz. Performance is impacted by conductor and dielectric losses as well as the excitation of higher-order modes. Despite that, the efficiency remains above 80% and makes the antenna suitable for 5G mmWave.

Figure 13. depicts the efficiency of the antenna over the frequency range. There is a small dip at 38 GHz, which is followed by an increase in efficiency at the higher frequency range. This is the result of the interaction of the modes and the impedance of the antenna. The observation is congruent with the slotted patch and the HR-DGS structure, which, through the electromagnetic design and optimization of the current distribution, enhances the performance and efficiency of the antenna.

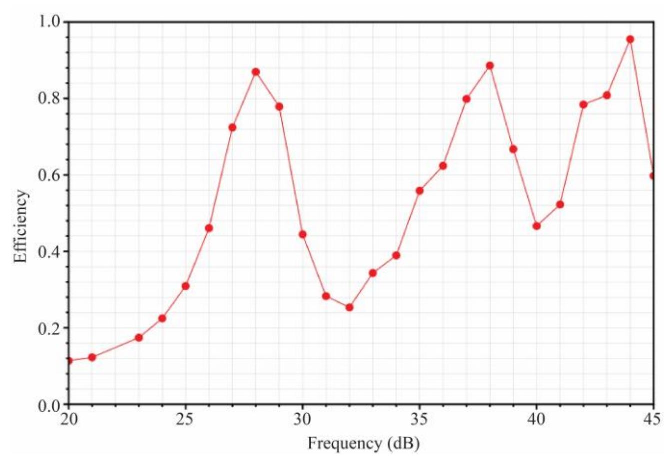

Fig. 13 Radiation efficiency of simulated design

5. Conclusion

This paper presents a new concept in the design and analysis of planar triple-band microstrip patch antennas for millimeter-wave 5G applications. Specifically, it focuses on an antenna design with an innovative Hybrid-Ring Defected Ground Structure (HR-DGS) design. The antenna operates at 28 GHz, 38 GHz, and 43 GHz. In addition, the design accommodates some of the important frequency bands in the 3GPP FR2 spectrum. The combination of an HR-DGS structure in the ground plane and the use of quad slots in the radiating patch was effective for manipulating surface current and achieving a multi-resonant structure, while still balancing size constraints. This was accomplished through the use of a Rogers RT/Duroid 5880 substrate and an optimized HR-DGS. Radiation pattern analyses were conducted, and based on the results, broadside radiation with clean main-lobe behavior was observed at 28 GHz. In addition, the antenna exhibited sufficient radiation behavior at the specified higher frequencies of 38 GHz and 43 GHz, with sufficient directivity and controlled higher-order modes. The proposed antenna, compared to the previously reported designs, exhibits a considerable reduction in size with a smaller footprint of 4 mm x 5 mm x 0.787 mm, with similar and competitive bandwidth and gain figures.

Acknowledgment

The authors would also like to take this opportunity to thank. The African Union (AU) for their invaluable contributions and willingness to support the advancement of scientific research and technological innovation throughout the continent. The AU Commission facilitated this work by providing the necessary resources and a workspace where this research could be conducted.

Table 4 Comparison of the present work with previously published work

References	Dimensions (mm×mm×mm)	Frequency (GHZ)	BW(GHz)	Gain(dBi)
[12]	12×12×0.237	28×38	4.5×3.8	4.54×4.421
[4]	4.95×5.8×0.25	28×38	0.6×0.6	7.37×8.13
[13]	7.5×8.8×0.25	28×38	1.2×1.1	6.62×5.81
[1]	4.8×5.5×0.25	28×38	0.5×0.6	7×6.5
[14]	5.99×5.99	29.5	13.75	5.8174
[15]	6.2×8.4×1,57	26×28	5.368×5.368	7.88×7.33
[16]	12.2×9.77×0.508	28×32×38	1×0.7×1.68	9.153×7.48×12.78
This Work	4×5×0.787	28×38×43	1.19×1.87×1.12	6.33×4.20×4.7

References

[1] R. A. Al-Atyar et al., "Dual-Band (28/38 GHz)–Loaded Patch Antenna for Millimeter-Wave Communication," *Journal of Infrared, Millimeter, and Terahertz Waves*, vol. 46, no. 3, 2025. [CrossRef] [Google Scholar] [Publisher Link]

[2] Theodore S. Rappaport et al., "Millimeter Wave Mobile Communications for 5G Cellular: It will Work," *IEEE Access*, vol. 1, pp. 335-349, 2013. [CrossRef] [Google Scholar] [Publisher Link]

[3] Tathababu Addepalli et al., "Super-Wide Band (25–43 GHz), 4-Element MIMO Antenna with High Diversity for 5G Mm Wave Advanced Wireless System Applications," *Wireless Personal Communications*, vol. 146, no. 3, pp. 1629-1666, 2026. [CrossRef] [Google Scholar] [Publisher Link]

[4] Rania R. Elsharkawy, F.A. Hussein Khalid, and Asmaa E. Farahat, "Dual-Band (28/38 GHz) Compact MIMO Antenna System for Millimeter-Wave Applications," *Journal of Infrared, Millimeter, and Terahertz Waves*, vol. 44, no. 11-12, pp. 1016-1037, 2023. [CrossRef] [Google Scholar] [Publisher Link]

[5] Daud Khan, Ashfaq Ahmad, and Dong-You Choi, "Dual-Band 5G MIMO Antenna with Enhanced Coupling Reduction using Metamaterials," *Scientific Reports*, vol. 14, pp. 1-16, 2024. [CrossRef] [Google Scholar] [Publisher Link]

[6] Youssef Frist, Mourad Elhabchi, and Mohamed Nabil Srifi, "28/38 GHz Antenna for Millimeter Wave 5G Applications with Radiation Pattern Reconfigurability Using CSRR and DGS," *Journal of Communications*, vol. 19, no. 9, pp. 441-448, 2024. [CrossRef] [Publisher Link].

[7] Parveez Shariff Bhadravathi Ghouse et al., "Dual-Band Antenna at 28 and 38 GHz Using Internal Stubs and Slot Perturbations," *Technologies*, vol. 12, no. 6, pp. 1-23, 2024. [CrossRef] [Google Scholar] [Publisher Link]

[8] Md. Amanath Ullah et al., "Low-Profile Dual-Band Pixelated Defected Ground Antenna for Multistandard IoT Devices," *Scientific Reports*, vol. 12, no. 1, pp. 1-19, 2022. [CrossRef] [Google Scholar] [Publisher Link]

[9] Ashok Kumar, Ashok Kumar, and Arjun Kumar, "Defected Ground Structure Based High Gain, Wideband and High Diversity Performance Quad-Element MIMO Antenna Array for 5G Millimeter-Wave Communication," *Progress in Electromagnetics Research B*, vol. 101, pp. 1-16, 2023. [CrossRef] [Google Scholar] [Publisher Link]

[10] Mamadou Mamarou Diallo, Dominic Bernard Onyango Konditi, and Olivier Videme Bossou, "A Miniaturized Dual-Band Planar Antenna with a Square Ring Defected Ground Structure for 5G Millimetre-Wave Applications," *Indonesian Journal of Electrical Engineering and Computer Science*, vol. 29, no. 1, pp. 197-205, 2023, [CrossRef] [Google Scholar] [Publisher Link]

[11] Sumeet Singh Bhatia, and Narinder Sharma, "A Compact Wideband Antenna Using Partial Ground Plane with Truncated Corners, L – Shaped Stubs and Inverted T – Shaped Slots," *Progress in Electromagnetics Research M*, vol. 97, pp. 133-144, 2020. [CrossRef] [Google Scholar] [Publisher Link]

[12] Ayman R Sabek, Ahmed A Ibrahim, and Wael A Ali, "Dual-Band Millimeter Wave Microstrip Patch Antenna with Stub Resonators for 28/38 GHz Applications," *Journal of Physics: Conference Series: 6th International Conference on Advanced Technology and Applied Sciences*, Cairo, Egypt, vol. 2128, pp. 1-10, 2021. [CrossRef] [Google Scholar] [Publisher Link]

[13] Asmaa E. Farahat, and Khalid F. A. Hussein, "Dual-Band (28/38 GHz) Wideband MIMO Antenna for 5G Mobile Applications," *IEEE Access*, vol. 10, pp. 32213-32223, 2022. [CrossRef] [Google Scholar] [Publisher Link]

[14] Awatef Djouimaa, and Karima Bencherif, "Design of a Compact Circular Microstrip Patch Antenna for 5G Applications," *Engineering, Technology and Applied Science Research*, vol. 14, no. 4, pp. 16020-16024, 2024. [CrossRef] [Google Scholar] [Publisher Link]

[15] Jawdat S. Alkasassbeh et al., "Design and Optimization of a Compact Inset Feed Microstrip Antenna for 5G Applications with Enhanced MIMO Performance," *Engineering, Technology and Applied Science Research*, vol. 15, no. 2, pp. 21373-21382, 2025. [CrossRef] [Google Scholar] [Publisher Link]

[16] Mouaaz Nahas, "A Multi-Slotted Multi-Band Microstrip Patch Antenna Design for 5G Communication Devices," *Engineering, Technology and Applied Science Research*, vol. 15, no. 4, pp. 24605-24610, 2025. [CrossRef] [Google Scholar] [Publisher Link]

[17] AbdulGuddoos S. A. Gaid, and Mohammed A. M. Ali, "Tri-Band Rectangular Microstrip Patch Antenna with Enhanced Performance for 5G Applications Using a π-Shaped Slot: Design and Simulation," *Iraqi Journal for Electrical and Electronic Engineering*, vol. 19, no. 2, pp. 179-190, 2023. [CrossRef] [Google Scholar] [Publisher Link]

[18] Rakesh N. Tiwari et al., "Triple Band Lateral 4-Port Flexible MIMO Antenna for Millimeter Wave Applications at 24/28/38 GHz," *Results in Engineering*, vol. 26, pp. 1-14, 2025. [CrossRef] [Google Scholar] [Publisher Link]

[19] Ruaa Shallal Abbas Anooz et al., "A G-Shape Slot Rectangular Microstrip Patch Antenna for Microwave Applications," *SSRG International Journal of Electrical and Electronics Engineering*, vol. 10, no. 6, pp. 43-49, 2023. [CrossRef] [Google Scholar] [Publisher Link]